




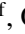
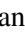



# Multi-Layer Energy Management System for Cost Optimization of Battery Electric Vehicle Fleets

Róbinson Medina<sup>1</sup><sup>a</sup>, Nikos Avramis<sup>1</sup><sup>b</sup>, Subhajeet Rath<sup>1</sup><sup>c</sup>, Mohammed Mahedi Hasan<sup>3</sup><sup>d</sup>,  
Dai-Duong Tran<sup>3</sup><sup>e</sup>, Zisis Maleas<sup>4</sup><sup>f</sup>, Omar Hegazy<sup>3</sup><sup>g</sup> and Steven Wilkins<sup>1,2</sup><sup>h</sup>

<sup>1</sup>Powertrains Department, TNO, The Netherlands

<sup>2</sup>Electrical Engineering, Eindhoven University of Technology, The Netherlands

<sup>3</sup>Electrical Engineering and Power Electronics, Vrije Universiteit Brussels, Belgium

<sup>4</sup>Operations Research, Centre for Research & Technology Hellas, Greece

**Keywords:** Energy Management System, Battery Electric Vehicle, Smart Charging, Vehicle Speed Advise, Vehicle Thermal Optimization, Vehicle Routing Problem.


**Abstract:** One of the biggest barriers for a wider adoption of Battery-Electric Vehicles (BEVs) is their relatively higher cost compared to their combustion-based alternatives. A potential solution is to develop Energy Management Systems (EMSs), which make a more efficient use of the vehicle energy, resulting in a cheaper operation. EMSs are commonly composed of algorithms operating at fleet and vehicle layers. For example, at fleet layer one can find *eco-routing* for optimising the vehicle route, and *eco-charging* for smart charging. Likewise, at vehicle layer one can find algorithms such as *eco-driving* for minimizing speed-related losses and *eco-comfort* for minimizing the thermal-components energy consumption. These eco-functions affect the operational cost of the fleet due to reduction of metrics such as energy consumption and travelling time (which impacts labor costs). This paper presents the development of a multi-layer EMS, which integrates the aforementioned fleet and vehicle-level eco-functions. The paper focuses on the energy and operational cost savings that such a multi-layer EMS can bring to a fleet owner. Simulation results show that the EMS saves on costs produced by travelling time and energy consumption. However, the ideal ratio between these savings ultimately depends on the region, as electricity price and labor costs vary greatly.


## 1 INTRODUCTION


Battery-Electric Vehicles (BEVs) are currently emerging as a viable replacement for Internal-Combustion Engine (ICE)-based vehicles in many transport sectors (Smith, 2010; Ewert et al., 2020). This replacement is mostly motivated by the environmental advantages that BEVs have, such as zero-tailpipe emissions and lower well-to-wheel emissions (Ahmadi, 2019; Gao et al., 2023). For some light-duty commercial applications, such as


last-mile deliveries, the current available BEVs are already a feasible alternative for ICE (Siragusa et al., 2022; Sendek-Matysiak et al., 2022). However, BEVs still face multiple challenges such as increased costs (compared to ICEs) (Anosike et al., 2023). This challenge can be partially overcome by the usage of Energy Management Systems (EMSs), which seek to make the operation of BEVs more efficient.


Commonly, EMSs are developed to optimize a single aspect of the vehicle operation. Such EMSs are found on fleet or vehicle layers. For example, when applied directly on the vehicle, one can find algorithms such as *eco-comfort* and *eco-driving*, which are focused on reducing the on-board energy consumption. Specifically, an EMS such as *eco-comfort* minimizes the energy consumption of all thermal components in the vehicle while *eco-driving* provides a speed advise for the driver which minimizes the energy consumption of the vehicle powertrain. Examples of such algorithms can be found in (Kwak


<sup>a</sup> <https://orcid.org/0009-0001-2214-6153>


<sup>b</sup> <https://orcid.org/0009-0007-3345-1018>


<sup>c</sup> <https://orcid.org/0000-0001-8655-0334>

<sup>d</sup> <https://orcid.org/0000-0001-7663-4948>

<sup>e</sup> <https://orcid.org/0000-0002-3593-0748>

<sup>f</sup> <https://orcid.org/0000-0003-1909-1259>

<sup>g</sup> <https://orcid.org/0000-0002-8650-7341>

<sup>h</sup> <https://orcid.org/0000-0001-9498-2321>

et al., 2023; Naeem, 2023; Medina et al., 2020). (Kwak et al., 2023) developed an *eco-comfort* algorithm that is based on a model predictive controller, to achieve energy savings up to 35%. (Naeem, 2023) designed a strategy that provides speed advice to the driver, to maximize the BEV range and battery health. Simulation results show energy improvements of up to 20%. (Medina et al., 2020) co-designed an *eco-comfort* and *eco-driving* for passenger-vehicles applications, showing that the individual savings of each eco function (partially) adds up to up to 7.1%.

Likewise, when the EMSs are applied on a fleet layer, the algorithms focus on organizing the fleet operations on an efficient way via algorithms such as *eco-routing* and *eco-charging*. *Eco-routing* produces vehicle routes that minimizes the traveling time of the whole fleet, while *eco-charging* provides a charging schedule that minimizes the total charging costs. Examples of such algorithms can be found in (Lera-Romero et al., 2024; Geerts et al., 2022; Zhang et al., 2021). (Lera-Romero et al., 2024) designed an *eco-routing* algorithm for last-mile deliveries which integrates variability in the vehicle energy consumption induced by the drive cycle. Simulation results show that the scope of unfeasible problems is reduced, due to the more precise prediction on energy consumption of the algorithm. (Geerts et al., 2022; Zhang et al., 2021) presented fleet-charging strategies for light-duty vehicles and electric busses, respectively, which minimized the operational costs due to electricity and battery degradation.

Combinations of these fleet-layer algorithms are also common. For example, (Cataldo-Díaz et al., 2024) presented a co-design of an *eco-routing* and *eco-charging* algorithm, where the latter enables the usage of the battery to its full capacity (i.e., 100% instead of only the fast charging range), which increases the efficiency of the routing problem. Likewise, (Lacombe, 2023) proposed a distributed optimization method to combine fleet-level driving strategies with charging strategies (i.e., *eco-driving* and *eco-charging*).

All of these EMSs show savings due to one or two algorithms operating exclusively in the fleet or vehicle layer. Only in our technical report (Medina et al., 2023), the energy interaction of all four mentioned eco-functions is described. To the best of the authors knowledge, the operational cost savings of the four mentioned eco-functions has not been shown before.

This paper presents the interactions of multiple algorithms in a multi-layer EMS for BEV fleets. The multi-layer EMS is composed of fleet (*eco-routing* and *eco-charging*) and vehicle layers (*eco-driving* and *eco-comfort*). The resulting interactions are described

not only on the potential of energy savings, but also in the total operational costs of using the EMS.

The remaining of this document is divided as follows. Section 2 describes the design of the multi-layer EMS. A realistic case study is described in Section 3, where multiple types of light-duty based deliveries are used; Section 4 shows simulation results where the interactions of the multi-layer EMS is analysed. The paper closes with conclusions in Section 5.

## 2 MULTI-LAYER EMS DESIGN

This section presents a summary of the design of the multi-layer EMS. The complete version of the design can be seen in (Medina et al., 2023). The multi-layer EMS is composed of two fleet-layer algorithms (*eco-charging* and *eco-routing*), together with two vehicle-layer algorithms (*eco-driving* and *eco-comfort*).

### 2.1 Eco-Charging Algorithm

#### 2.1.1 General Description of *eco-charging*

The objective of *eco-charging* algorithm is to generate a charging schedule for a fleet of BEVs, while reducing the charging-related costs. The charging schedule refers to the charging power profile for each vehicle in a fleet within a time window. The algorithm fulfills multiple objectives such as completing the charging operation within a charging window and reaching a target State-of-Charge (SoC) before the vehicle departure while, adhering to grid/charger capacity constraints.

Fig. 1 shows a schedule for a fleet of  $N$  BEVs in a charging depot, where the time-slot available for charging is marked in green. During this window of opportunity, vehicle  $i$  must be charged from an initial SoC ( $\bar{z}^i$ ) to a target SoC ( $\bar{z}^i$ ). The output of *eco-charging* algorithm is the charging power ( $P_c$ ) per vehicle and time slot that can be drawn from the charger.

#### 2.1.2 Mathematical Formulation of *eco-charging*

The complete mathematical formulation for the problem statement can be found in (Rath et al., 2023), where the optimization problem for *eco-charging* is defined as

$$\min_{P_c} \quad \mathcal{J}_{el} + \mathcal{J}_{ca} + \mathcal{J}_{cy} \quad (1a)$$

$$\text{s.t.} \quad \sum_{i=1}^N P_c \leq \hat{P}_G, \forall j \in \mathbb{T} \quad (1b)$$

$$\mathbf{P}_c \in \{\{0\} \cup \{[\underline{P}_c, \bar{P}_c]\}\}^n \quad (1c)$$

$$\bar{z}^i \leq z^i \leq 1, \forall i \in \mathbb{V}, \quad (1d)$$

Time	09:00	09:15	09:30	...	$j$	...	20:00	20:15	20:30
Vehicle 1			$\underline{z}^1$					$\bar{z}^1$	
Vehicle 2	$\underline{z}^2$						$\bar{z}^2$		
Vehicle $i$		$\underline{z}^i$						$\bar{z}^i$	
Vehicle N				$\underline{z}^N$					$\bar{z}^N$

 Figure 1: Overview of *eco-charging* algorithm.

The objective of Eq. 1 is to minimize the cost of operation during fleet charging. In this work, the cost due to electricity from the grid ( $J_{el}$ ) and cost due to battery degradation as cyclic and calendar aging ( $J_{ca}$  and  $J_{cy}$ ) are considered in the objective function. Note that there might be other charging-related costs such as the ones related to charging losses operation or grid-related costs (Donateo et al., 2014; Geerts et al., 2022). Including these costs remains an open research question.

The cost of electricity from the grid is

$$J_{el} = \mathcal{E}_{el} \cdot \varepsilon_c \cdot \mathbf{P}_c \cdot \Delta t_c, \quad (2)$$

where  $\mathcal{E}_{el}$  is the time-varying price of electricity,  $\mathbf{P}_c$  is the vector of charging power at every available time-slot,  $\varepsilon_c$  is the efficiency of charging from grid-to-vehicle and  $\Delta t_c$  is the length of a time-slot in hours.

The battery degradation cost is given by

$$J_{ca} = \mathcal{E}_{bat} \cdot a_1 \cdot \mathbf{z} \cdot 10^6 \cdot e^{-a_3/T_P} t^{0.75} / \tilde{C}_B^{eff}, \quad (3)$$

$$J_{cy} = \mathcal{E}_{bat} \cdot b_4 \cdot (\mathbf{P}_c / \bar{C}_B) \cdot \sqrt{Q} / \tilde{C}_B^{eff}. \quad (4)$$

where  $\mathcal{E}_{bat}$  is the effective battery cost,  $\mathbf{z}$  is the vector of SoC at every available time-slot,  $T_P$  and  $t$  are the battery pack temperature and time elapsed for calendar aging,  $\bar{C}_B$  and  $Q$  are maximum battery capacity and charge throughput during cyclic aging and  $\tilde{C}_B^{eff}$  is the required capacity drop (normalized) after which the battery is considered at its End-of-Life (EoL).  $a_x$  and  $b_y$  are battery-specific aging parameters.

Let  $\mathbb{V}$  and  $\mathbb{T}$  be a set of all vehicles and time-slots. Variable  ${}^i_j P_c \in \mathbf{P}_c$  can be defined as the charge power for vehicle  $i \in \mathbb{V}$  at time-slot  $j \in \mathbb{T}$ .

The optimization problem is subject to three constraints. Eq. 1b describes the constraint due to grid capacity where the total power drawn by the vehicle at every time-slot must be below the maximum power supplied by the grid to the vehicle ( $\hat{P}_G$ ).  $\hat{P}_G$  takes into account the charging efficiency and scales the grid capacity to vehicle level. Eq. 1c limits the charging power between  $\underline{P}_c$  and  $\bar{P}_c$  during the charging process while at rest it is set to 0. Here,  $\underline{P}_c$  and  $\bar{P}_c$  are the minimum and maximum charging power of the charger. Eq. 1d constrains the vehicle SoC to reach the target SoC without exceeding 1.

The algorithm assumes that the number of chargers is equal to the number of vehicles. The charging characteristics of the battery are considered linear, i.e., the SoC increases proportionally with the charge power. It is also assumed that the charging window and initial and target SoC are known in advance and that a charging event cannot be interrupted once started. Further details about the *eco-charging* implementation are given in (Rath et al., 2023).

## 2.2 Eco-Routing Algorithm

### 2.2.1 General Description of *eco-routing*

The objective of *eco-routing* algorithm is to generate the optimal route that a delivery vehicle must follow to minimize energy consumption of the fleet. The problem is constrained by battery and payload capacity, completion of all deliveries within a stipulated time and ensuring the the vehicle has adequate charge to complete the delivery route. Such problems are defined under the broader category of Vehicle Route Problems (VRPs), which are computationally NP-Hard (nondeterministic polynomial time). In this work, an advanced Mixed Integer Optimization Problem (MIP) technique (branch and cut) is used to improve the execution time of the optimizer, as described in (Kallehauge et al., 2005).

### 2.2.2 Mathematical Formulation of *eco-routing*

A graph  $G = (V, A)$  is defined where  $V$  is the set of stops and  $A$  is the set of Arcs (connecting the stops).  $c_{ij}$ ,  $f_{ij}$  and  $t_{ij}$  are defined as consumption (kWh), load (parcels) and time (minutes) when the vehicle moves from stop  $i$  to  $j$ .  $Q$  is the maximum capacity of the vehicle and  $r$  time available to recharge the vehicle. A variable  $x_{ij}$  can be defined as

$$x_{ij} = \begin{cases} 1, & \text{If vehicle moves from stop } i \text{ to } j \\ 0, & \text{Otherwise.} \end{cases}$$

The optimization problem is formulated as a VRP with a single time window, battery and capacity constraints and charging operations as

$$\min_x \sum_{i \in V} \sum_{j \in V} c_{ij} x_{ij} \quad (5a)$$

$$\text{s.t.} \quad \sum_{i \in V} x_{ij} = 1, \quad \forall j \in V, i \neq j \quad (5b)$$

$$\sum_{j \in V} x_{ij} = 1 \quad \forall i \in V, i \neq j \quad (5c)$$

$$\sum_{i \in V} x_{0j} \geq \lceil |N|/Q \rceil \quad (5d)$$

$$\sum_{j \in V} x_{0j} = \sum_{j \in V} x_{j0} \quad (5e)$$

$$f_{ij} \leq Qx_{ij}, \quad \forall i \in V, i \neq j \quad (5f)$$

$$\sum_{j \in V/0} f_{0j} - \sum_{j \in V/0} f_{j0} \geq -Q \quad (5g)$$

$$\sum_{j \in V, i \in V, i \neq j} x_{ij}t_{ij} \leq 480 - 30r \quad (5h)$$

$$\sum_{j \in V, i \in V, i \neq j} x_{ij}c_{ij} \leq 0.8 + 0.3r \quad (5i)$$

$$\sum_{j \in V, i \in V, i \neq j} x_{ij} \leq |S| - 1, \quad \forall S \subseteq V/\{0\}. \quad (5j)$$

The objective function of Eq. 5a minimizes the total energy consumption by reducing the total driven distance. Eqs. 5b, 5c and 5e ensure that the vehicle enters a node (request) and after dropping the order, exits the node. Eq. 5d forces the vehicle to go to the depot at least as many times as needed based on load capacity constraints. Eqs. 5f and 5g ensure that the vehicle does not exceed the capacity of the cargo body and during every visit to the depot it can be loaded with up to the available capacity, respectively. Eq. 5h ensures that the total driving time and charging time are not more than a time window of 8 hours (480 minutes). Similarly, Eq. 5i ensures that the SoC at the start of the route and the additional charging that may be performed during the day are enough to complete the route. Finally, Eq. 5j is the subtour elimination constraint. Subtours are paths that visit a subset of nodes, without circling back to the depot.

## 2.3 Eco-Driving Algorithm

### 2.3.1 General Description of *eco-driving*

The goal of the *eco-driving* algorithm is twofold: first, to provide a speed advice to the driver and second to provide *eco-comfort* with a prediction of the traction power consumption for a certain period ahead.

The *eco-driving* algorithm uses an offline heuristic way to determine the maximum acceleration and deceleration of the vehicle. Using an offline heuristic eases implementation, as it does not require a powerful computational platform or online data connectivity for prediction information. However, as all the data is precomputed, changes along the drive cycle result in suboptimal solutions.

The heuristic algorithm generates a smooth speed profile without high power peaks, which leads to energy savings (Han et al., 2019; Ajanović et al., 2018). Additionally, the maximum speed of the vehicle is limited to further obtain energy savings, which is specially relevant in an urban environment.

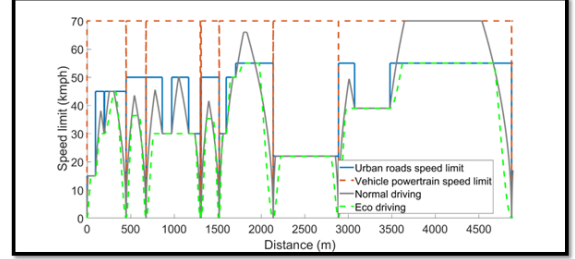


Figure 2: Optimal and regular driving speed limits.

However, these rules result in an increased travelling time for the BEV, creating a trade-off is between energy savings and travelling time. Fig. 2 shows an example of how the speed limits are adjusted due to *eco-driving* and also how the acceleration profile is affected.

### 2.3.2 Mathematical Formulation of *eco-driving*

The inputs from *eco-driving* include a vector of coordinates with latitude and longitude ( $\vec{\phi}, \vec{\lambda}$ ) and a vector of speed limits  $\vec{v}_{lim}$  along the upcoming trip. An overview of *eco-driving* can be seen in Fig. 3. *Eco-driving* uses these inputs to create an optimal speed profile  $\vec{v}_{opt}$ , following the next steps:

1. Create a distance profile  $\vec{\Delta}_d$  per input coordinate. Each point in distance vector  $\Delta_{d,i}$  is calculated using the Haversine formula:

$$\Delta_{d,i} = 2r \sin^{-1} \left( \sin^2 \left( \frac{\Delta\phi_i}{2} \right) + \cos(\phi_i) \cos(\phi_{i+1}) \cos^2 \left( \frac{\Delta\lambda_i}{2} \right) \right)^{0.5}, \quad (6)$$

where  $r$  is the Earth radius,  $\phi_i \in \vec{\phi}$ ,  $\Delta\lambda_i = \lambda_{i+1} - \lambda_i$ , and  $\Delta\phi_i = \phi_{i+1} - \phi_i$ , with  $i = [1, \dots, |\vec{\phi}|]$ .

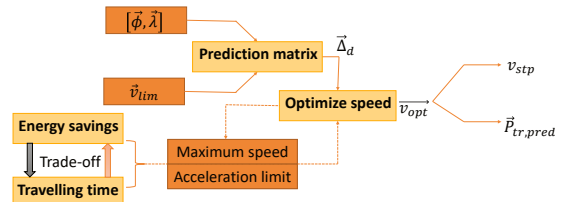


Figure 3: *Eco-driving* topology overview.

2. An acceleration vector  $\vec{a}_{tmp}$  is computed using the kinematics equation  $a_{tmp,i} = \frac{v_{lim,i+1}^2 - v_{lim,i}^2}{2\Delta_{d,i}}$ , with  $a_{tmp,i} \in \vec{a}_{tmp}$ ,  $v_{lim,i} \in \vec{v}_{lim}$  and  $i = [1, \dots, |\vec{a}_{tmp}|]$ .
3. A new acceleration vector  $\vec{a}$  is computed using an acceleration limit  $\bar{a}$ . That is,  $a_i = \max(a_{tmp,i}, \bar{a})$ ,  $a_i = \min(a_{tmp,i}, -\bar{a})$ , with  $a_i \in \vec{a}$ .
4. An intermediate velocity vector  $\vec{V}_{int}$  is calculated using  $\vec{a}$  and the kinematic equation from step 2.
5. A velocity vector  $\vec{V}_{fin}$  is computed by limiting  $\vec{V}_{int}$  to speeds up to  $\bar{V}$ , i.e.,  $V_{fin,i} = \max(V_{int,i}, \bar{V})$  with  $V_{fin,i} \in \vec{V}_{fin}$ .
6. A duration vector  $\vec{t}$  is created using the kinematic equation  $\Delta t_i = 2\Delta_{d,i} / (V_{fin,i+1} + V_{fin,i})$ , where  $t_i = t_{i-1} + \Delta t_i$  and  $t_i \in \vec{t}$ .
7. The energy requirements of the drive cycle are then computed. To do so, the traction force  $F_{tr}$  is computed using:

$$F_{tr} = \frac{1}{2}\rho c_d A_f v_{fin,i}^2 + c_r mg \cos(\alpha) + mg \sin(\alpha) + ma_i, \quad (7)$$

where  $\rho$ ,  $c_d$ ,  $A_f$ ,  $c_r$ ,  $m$  and  $\alpha$  are the air density, air drag, frontal area, rolling resistance, vehicle mass and road grade, respectively. The traction power  $\vec{P}_{tr,pred}$  and energy  $\vec{E}_{tr,pred}$  are computed as:

$$\vec{P}_{tr,pred} = F_{tr} \vec{v}_{fin}, \quad \vec{E}_{tr,pred} = \int \vec{P}_{tr,pred} dt. \quad (8)$$

8. Using  $E_{tr,pred}$  and  $\vec{t}$ , the trip energy consumption and traveling time can be evaluated. In case they are not satisfactory, steps 3-7 are to be recomputed using new values for  $\vec{a}$  and  $\vec{v}$ . A satisfactory result depends on the particular use case, as it will be shown in Section 3.3. Once the result is satisfactory, the optimal speed vector is defined as

$$\vec{V}_{opt} = \vec{V}_{fin}.$$

$\vec{V}_{opt}$  then is used as speed setpoint for the driver  $v_{stp}$ , which is updated during the drive cycle.

## 2.4 Eco-Comfort Algorithm

### 2.4.1 General Description of *eco-comfort*

The *eco-comfort* algorithm provides temperature setpoints for the thermal systems of the vehicle, namely the cabin, refrigerated cargo (if applicable) and the battery pack. To reduce execution time and guarantee an optimal solution, the algorithm uses convex models for all energy-consuming vehicle components. Additionally, the algorithm leverages weather forecast data, as well as the traction power profile estimated in *eco-driving*, to minimize the energy consumption of the thermal systems over a time horizon.

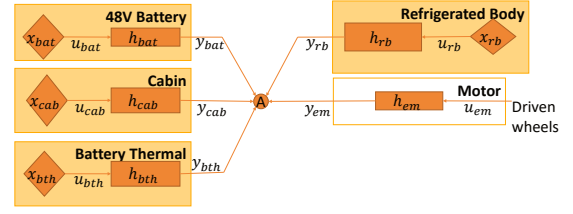


Figure 4: *Eco-comfort* topology overview.

### 2.4.2 Mathematical Formulation of *eco-comfort*

The vehicle components that consume electrical energy are first defined. The basic modelling principle is described by the power exchange among such components. Fig. 4 shows this power exchange.

The system consists of energy buffers ( $x$ ) and power converters ( $h$ ). Node A represents the interconnection for subsystems in the electrical power domain, e.g., the high-voltage bus. The sub indexes  $\mathcal{M} = \{bat, rb, cab, bth, em\}$  describe the subsystems of the vehicle: the battery (*bat*), cabin (*cab*), refrigerated body (*rb*), electric motor (*em*) and the thermal system of the battery (*bth*).

To formulate a convex optimization problem, the relationship between an input ( $u_m$ ) and output ( $y_m$ ) power in each subsystem, which represents the power losses, is written in a quadratic form:

$$y_m + \frac{1}{2} q_m u_m^2 + f_m u_m + e_m = 0, \quad (9)$$

with  $m \in \mathcal{M}$ ,  $q_m$ ,  $f_m$  and  $e_m$  are parameters.

The following states are defined:  $x_{bat}$  is the battery charge, while  $x_{rb}$ ,  $x_{cab}$  and  $x_{bth}$  are the stored thermal energies in the refrigerated body, further described as:

$$x_{n,k+1} = A_n x_{n,k} + B_n u_{n,k} + B_{d,n} d_{n,k}, \quad (10)$$

where  $n \in \{bat, rb, cab, bth\}$ ,  $A_n$ ,  $B_n$  and  $B_{d,n}$  are the state, input and input disturbance matrices,  $d_{n,k}$  a disturbance,  $k$  is the time instant index.

The objective of the optimization is to reduce battery energy consumption, while preserving passenger thermal comfort. The objective function is defined as:

$$\min_{u_{n,k}} \sum_{k \in K} w_1 u_{bat,k} + w_2 (T_{cab} - T_{cab,sp})^2 \quad (11a)$$

$$+ w_3 (T_{rb} - T_{rb,sp})^2 + w_4 (T_{bth} - T_{bth,sp})^2$$

$$\text{s.t. } X_{n,k+1} = A_n X_{n,k} + B_n U_{n,k} + B_{d,n} D_{n,k} \quad (11b)$$

$$\underline{X} \leq X_k \leq \bar{X} \quad (11c)$$

$$\underline{U} \leq U_k \leq \bar{U} \quad (11d)$$

$$y_{cab,k} + y_{bth,k} + y_{rb,k} + y_{em,k} + y_{bat,k} = 0 \quad (11e)$$

$$y_{m,k} + \frac{1}{2} q_m u_{m,k}^2 + f_m u_{m,k} + e_{m,k} \leq 0. \quad (11f)$$

With  $T$  denoting temperature and the subscript  $sp$  indicating a setpoint.

In the cost function, Eq. 11b corresponds to the previously defined first-order dynamics for each subsystem. The capital letters in states, inputs and disturbances (i.e.,  $X, U$  and  $D$ ) indicate the aggregated subsystems over the time horizon. Eqs. 11c and 11d denote constraints on upper and lower bounds for states ( $\underline{X}, \bar{X}$ ) and inputs ( $\underline{U}, \bar{U}$ ). The power interconnection at node A of Fig. 4 is captured in Eq. 11e. Finally, the quadratic relationship of Eq. 9 is captured in Eq. 11f. Notice that Eq. 11f has been relaxed to an inequality to ensure convexity.

The weighing factors  $w_1$ - $w_4$  are calibrated heuristically, to obtain energy savings while keeping cabin in an acceptable range for the passenger.

### 3 CASE STUDY

This section presents a motivational case study, where the multi-layer EMS is applied.

#### 3.1 Vehicle Fleet

A fleet of 11 BEVs is considered, to carry out different delivery routes, under multiple weather conditions, and create a realistic operation for evaluating the multi-layer EMS. To do so, each one of the vehicles drives one test case with a different route, weather conditions or settings for *eco-comfort*. An overview of the test cases is shown in Table 1.

The fleet of vehicles is assumed to be carrying out simultaneously two types of last-mile delivery operations: post-delivery and food-delivery case. Both last-mile deliveries are performed out in city environments. All deliveries are carried out during day time while all charging is carried out during nighttime. The post-delivery test case is assumed to be carried out in 3 different routes across Belgium. Such deliveries show frequent stops to deliver packages, and the weather conditions vary around  $5^\circ\text{C}$ . An example of the prediction data is shown in Fig. 5. The low-speed instances (i.e., when the speed is less than 10 km/h) denote delivery locations.

The food-delivery use case is executed in Thessaloniki, Greece. An example of the prediction data on this use case is shown in Fig. 6. It can be seen that the delivery of food requires fewer stops than those of the post. Likewise, due to the location, the weather conditions show relatively warmer temperatures (above  $30^\circ\text{C}$ ) compared to post-delivery operation. These differences in weather conditions are taken to show the difference between winter and sum-

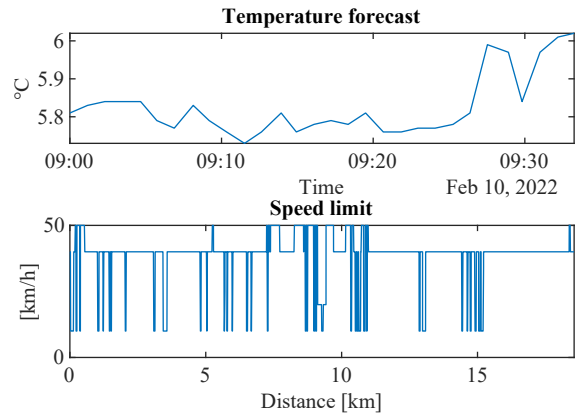


Figure 5: Prediction data example of test case 12. Data obtained using the APIs described in (Medina et al., 2023).

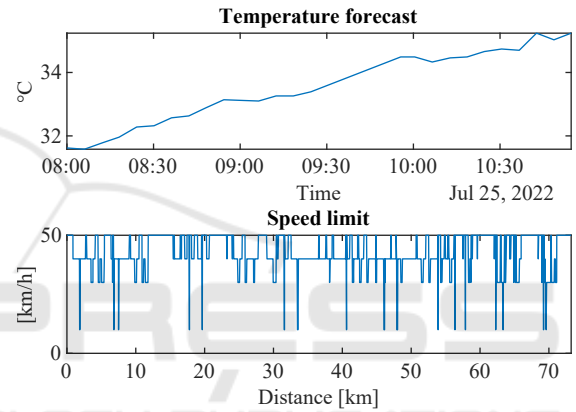


Figure 6: Prediction data example of test case 2. Data obtained using the APIs described in (Medina et al., 2023).

mer operations. Note that last-mile delivery is specially relevant for the multi-layer EMS, as the required frequent stops in the city environment gives ample opportunity for route and energy consumption optimization. Other use cases with similar opportunities might also be of interest.

#### 3.2 Vehicle Modelling

To evaluate the energy consumption for every test case defined in the previous section, a vehicle model and a powertrain model are created. The models correspond to an N1-category BEV, which is commonly used for urban deliveries. Such models follow forward-facing dynamics, as shown for example in (Medina et al., 2020). The model parameters are adapted for an N1-category vehicle. The vehicle and powertrain models are operated by a driver model which is a controller that follows a reference speed. Such a reference is taken as the road speed limit or the advised speed from *eco-driving*.

Table 1: Test cases description.

ID	Location	Goal
2	Greece	Summer thermal savings, passenger comfort setting 1, benchmark cabin temp at 20°
3	Greece	Summer thermal savings, passenger comfort setting 2, benchmark cabin temp at 20°
4	Greece	Summer thermal savings, passenger comfort setting 3, benchmark cabin temp at 20°
5	Greece	Summer thermal savings, passenger comfort setting 1, benchmark cabin temp at 22°
6	Greece	Summer thermal savings, passenger comfort setting 2, benchmark cabin temp at 23°
7	Greece	Summer thermal savings, passenger comfort setting 3, benchmark cabin temp at 23°
8	Belgium 1	Winter thermal savings, passenger comfort setting 1, benchmark cabin temp at 20°
9	Belgium 1	Winter thermal savings, passenger comfort setting 2, benchmark cabin temp at 20°
10	Belgium 1	Winter thermal savings, passenger comfort setting 3, benchmark cabin temp at 20°
11	Belgium 2	Eco-comfort validation, passenger comfort setting 2
12	Belgium 3	Eco-driving energy savings in urban environment

### 3.3 Simulation Environment

To quantify the multi-layer EMS benefits, a simulation environment is designed in Matlab (Medina et al., 2023). The simulation environment splits the problem into online and offline parts, as Fig. 7 shows.

The offline part runs the fleet-layer eco-functions (*eco-charging* and *eco-driving*) to generate charge planning and driving routes for the whole fleet. The eco-functions take inputs from the logistic assignment, such as delivery locations or required SoC at the start of the day. Given the generated routes and charging schedule, APIs are used to predict traffic information (e.g., the speed limit, road grade) and weather forecast (e.g., temperature forecast) along the traveled routes of the vehicle (see for example Fig. 6).

The online part runs a vehicle model while taking as input the output of the offline part. For example, the road grade affects the vehicle dynamics, and the temperature forecasts the thermal losses. Likewise, *eco-driving* and *eco-comfort* run in the online part. For each time step in the simulation, the temperature setpoints and speed advice are provided for the vehicle models to follow. The resulting relevant metrics are recorded (e.g., traveling time, energy consumption) and used to evaluate the EMS performance.

### 3.4 Performance Metrics

The multi-layer EMS is compared using two relevant metrics: energy consumption and total cost of operation. Energy consumption is recorded directly from the battery and normalized for the number of traveled kilometers along that route. Note that the on-board eco-functions are designed to minimize this metric.

The total operational costs are considered as the result of energy prices, labor, and battery degradation, i.e.:

$$\mathbf{C} = \mathcal{J}_{el} + \mathcal{J}_{ca} + \mathcal{J}_{cy} + \mathcal{J}_l, \quad (12)$$

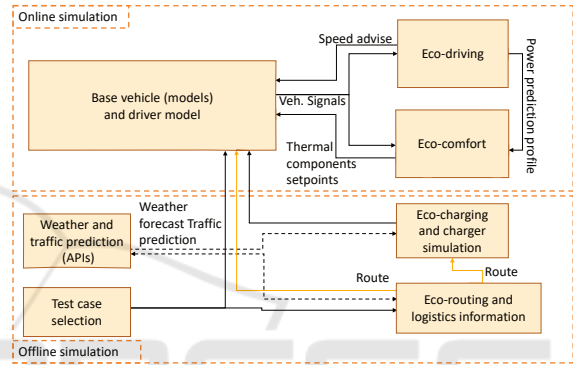


Figure 7: Simulation environment overview.

where  $\mathbf{C}$  is the total cost in [€],  $\mathcal{J}_{el}$  is the electricity cost defined in Eq. 2,  $\mathcal{J}_{ca}$  and  $\mathcal{J}_{cy}$  are the calendar and cyclic ageing of the battery, respectively, further defined in Eqs. 3 and 4, and  $\mathcal{J}_l$  the labour cost given by

$$\mathcal{J}_l = T_l C_d, \quad (13)$$

where  $T_l$  is the total traveling time along the route and  $C_d$  is the driver hourly rate in [€/hour].

To compare the performance of each eco-function, a benchmark simulation is run. For *eco-routing* the benchmark corresponds to running the same logistic assignment based on a commonly-used heuristic algorithm that solves a Traveling Salesman Problem. For *eco-charging*, the benchmark corresponds to applying a greedy charging strategy (i.e., charge as soon as arrival to the depot). For the on-board eco-functions, the benchmark corresponds to running the routes provided by *eco-routing*, while not using the output of the on-board eco-functions. That is, the driver follows the speed limit, while the thermal systems follow a fixed temperature setpoint.

To compare the improvements achieved by the multi-layer EMS, the increase or decrease of cost is calculated as

$$\Delta \mathbf{C} = \frac{\mathbf{C}_{benchmark} - \mathbf{C}_{EcoFun}}{\mathbf{C}_{benchmark}} 100 [\%], \quad (14)$$

where  $C_{benchmark}$  and  $C_{EcoFun}$  are the operational costs [€] related to the benchmark and eco-functions scenarios, respectively, and  $\Delta C$  is the percentage of increase/decrease in total operational costs.

### 3.5 Multi-Layer EMS Parameters

To quantify the performance of the multi-layer EMS, some parameters need to be assumed.

For *eco-driving*, the maximum vehicle acceleration without the eco-function (i.e., in the benchmark scenario) is taken as  $a = 0.66m/s^2$  from (Purnot et al., 2021). Therefore, maximum acceleration profile with *eco-driving* is assumed as  $\bar{a} = 0.37m/s^2$  in test cases 2-11, and  $\bar{a} = 0.25m/s^2$  in test cases 11 and 12.

In *eco-comfort*, the weight factors  $w_1-w_4$  are chosen to give several saving settings: setting 1 corresponds to an “aggressive” profile (highest savings), setting 2 to a “moderate” one (middle savings) and setting 3 to a “smooth” one (lowest savings, maximum passenger comfort).

For *eco-charging*, the electricity price  $\mathcal{E}_{el}$  is 0.335 [€/kWh] from 23:00 to 07:00, and 0.385 [€/kWh] for the rest (Rath et al., 2023).

For the cost evaluation, the prices of labour rates are assumed as

$$C_d = 20 \left[ \frac{\text{€}}{\text{hour}} \right]. \quad (15)$$

This price falls within the range of labour cost in the European Union (European Commission, 2022). Notice that driver costs has more weight than those of electricity in the total cost calculation, as every saved hour accounts for much more than every kWh saved.

## 4 SIMULATION RESULTS

This section presents the results of simulating the multi-layer EMS with the case study of Section 3.

### 4.1 Fleet-Layer Savings of Eco-Functions

*Eco-routing* is applied for case study of Section 3, where the algorithm was able to compute a feasible route for each one of the test cases. As discussed in Section 2.2, the main goal of the algorithm is to reduce the total traveling distance. This is shown in Fig. 8 where the optimized traveling distance is always lower than the benchmark. The improvement is mostly visible in the test cases 8 to 10, as these relate to post-delivery cases which has a higher density

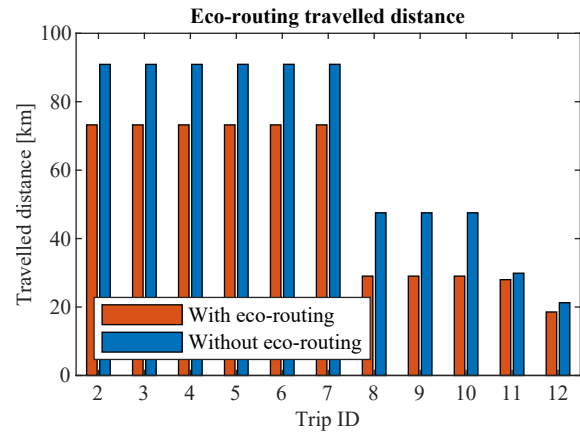


Figure 8: Travelled distance comparison with *eco-routing*.

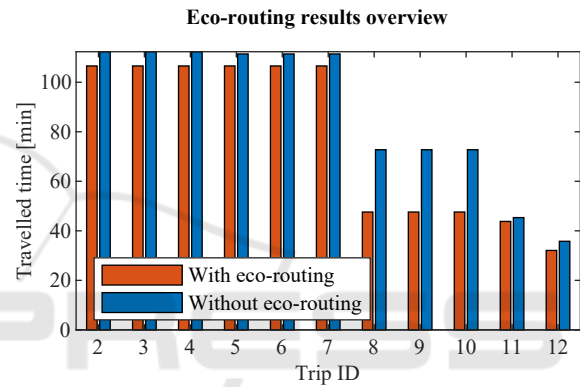


Figure 9: Travelled time comparison with *eco-routing*.

of deliveries compared to food-delivery. This creates more optimization opportunities for the parcel order.

Using the simulation environment proposed in Section 3.3, the proposed routes are simulated for different test cases without enabling on-board eco-functions. The resulting traveling times are shown in Fig. 9. As expected, the traveling time is shorter due to the shorter routes, which results in a reduction of operational costs, as subsequent paragraphs show.

Using the energy requirements provided by *eco-routing*, the *eco-charging* algorithm is run on the entire fleet. The resulting charged energy is seen in Fig. 10. Note that the charged energy while using *eco-charging*, already includes the effects of using *eco-driving* and *eco-comfort*. Therefore, using *eco-charging* results in less energy needed to be charged to each vehicle in the fleet.

Considering that the cost function of *eco-charging* reduces the total charging-related costs, the benefits of this algorithm are reflected in the economic savings. This is shown in Table 2. Due to the variable electricity price, *eco-charging* tends to charge the fleet when the energy price are lower. Likewise,



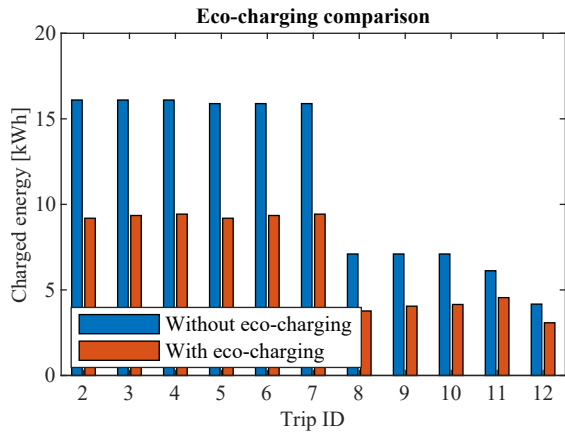
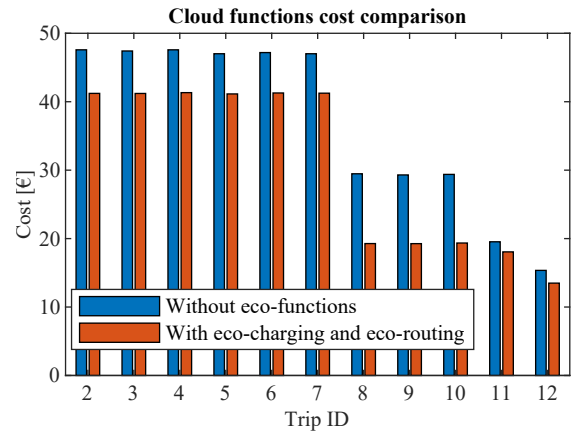

 Figure 10: Charged energy comparison with *eco-charging*.


Figure 11: Cost comparison with fleet layer eco-functions.

Table 2: Cost savings from eco-charging.

ID	Benchmark [€]			Eco-charging [€]			[%]
	$J_{el}$	$J_{cy}$	$J_{ca}$	$J_{el}$	$J_{cy}$	$J_{ca}$	
2	5.7	2.2	2.2	3.25	0.96	1.48	43.9
3	5.7	2.2	2.0	3.31	0.98	1.39	43.1
4	5.7	2.2	2.2	3.34	1	1.46	42.9
5	5.6	2.1	2.0	3.25	0.96	1.4	43.1
6	5.6	2.1	2.2	3.31	0.98	1.46	42.6
7	5.6	2.1	2.0	3.34	1	1.38	42.1
8	2.5	0.6	2.0	1.34	0.25	1.82	34.7
9	2.5	0.6	1.8	1.44	0.28	1.68	32.9
10	2.5	0.6	1.9	1.47	0.29	1.73	32
11	2.1	0.5	1.7	1.61	0.33	1.52	21.5
12	1.4	0.2	1.6	1.09	0.19	1.52	18.4

using the insights of the aging model on the battery, the algorithm achieves less deterioration in the battery lifetime compared to the benchmark strategy. This is more significant in terms of cyclic aging  $J_{cy}$ , as it seems to have a larger impact on the battery lifetime. This reduction corresponds to a reduction of at least 20% of costs in all test cases.

A total cost comparison of the cloud-based eco-functions is shown in Fig. 11. The total operational costs are always lower. Note that the electricity cost  $J_{el}$  is not taken into account in Fig. 11, as this is the result of the combined effect of using the on-board eco-functions and *eco-charging*. The electricity cost is therefore going to be considered in the on-board eco-functions, in the next subsection.

## 4.2 Vehicle-Layer Savings of Eco-Functions

Using the vehicle model of Section 3.2, the routes provided by *eco-routing*, and the traffic and weather prediction information provided by the APIs described in Fig. 7, the onboard eco-functions are tested

Table 3: On-board energy consumption in [kWh/km].

ID	No eco-functions	With <i>eco-driving</i>	With <i>eco-comfort</i> and <i>eco-driving</i>
2	0.137	0.135	0.126
3	0.137	0.135	0.128
4	0.137	0.135	0.129
5	0.133	0.131	0.126
6	0.133	0.131	0.128
7	0.133	0.131	0.129
8	0.149	0.145	0.13
9	0.149	0.145	0.14
10	0.149	0.145	0.143
11	0.188	0.165	0.163
12	0.197	0.169	0.166

on each one of the case studies of Table 1. As described in Section 2, the onboard eco-functions minimize energy consumption while driving the vehicle. An overview of the energy savings is shown in Table 3. Note that in each one of the trips, the energy consumption per kilometer is lower than while driving without using the eco-functions.

For the case of *eco-comfort*, although it produces savings on all cases, the largest savings appears under setting 1 (aggressive), which corresponds to test cases 2, 5, and 8. The lowest savings corresponds to setting 3 (smooth), which are cases 4, 7 and 10. Table 3 also shows relatively larger savings during winter than during summer. See for example the savings of test case 2 (summer) and test case 8 (winter). These larger savings are due the vehicle being equipped with an air conditioning for cooling and an electric resistance for heating. An air conditioning requires less energy to create the same difference in temperature than a resistor due to its Coefficient of Performance, resulting in more saving possibilities during winter. Note that *eco-comfort* does not affect traveling time

as it does not influence the driving dynamics.

*Eco-driving* provides the largest amount of savings in test cases 11 (12%) and 12 (14%), compared to the rest of the test cases (on average 2.9%). This is because in the test cases 11 and 12, the speed advice is built with the extra saving setting for limiting the acceleration, in contrast with the acceleration of the other test cases. This test case shows the large potential of energy savings that *eco-driving* has.

However, the energy savings produced by *eco-driving* come at the cost of extra traveling time, as shown in Fig. 12, which increases the labor costs. For example, test case 12 increases the traveling time by 25.9%, while the rest of the test cases increase it by on average 8.2%. This creates a trade-off between the savings on energy and the ones on labor: larger savings on energy result in added traveling time which creates labor costs. The acceleration limit and maximum speed of *eco-driving* need to be carefully chosen for each particular test case, to provide total operational savings.

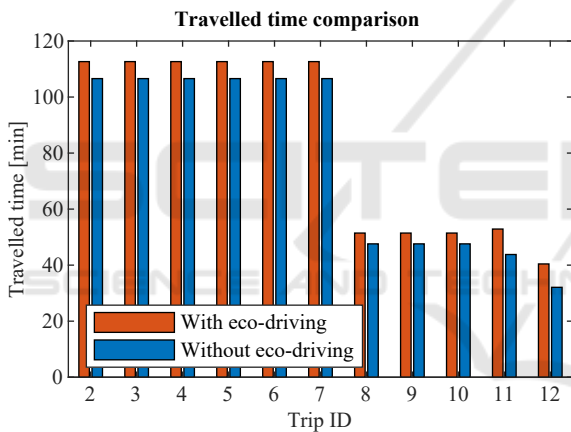


Figure 12: Travelled time comparison of *eco-driving*.

Using the rates presented in Section 3.5, the costs presented in Fig. 13 are calculated. Note that despite the combined energy savings of *eco-comfort* and *eco-driving*, the total operational cost per test case is virtually the same in most test cases, except for test cases 11 and 12. This is because the extra traveling time produced by *eco-driving* is canceling the effect of the energy savings, due to the driver rates being more significant than the electricity price. This is also partially because the charging operation occurs with low electricity prices, which is a result of using *eco-charging*. Notice that in test cases 11 and 12, the total cost of the eco-functions remains higher than the benchmark, because *eco-driving* produces significantly more traveling time. *Eco-driving* could become cost-effective if the electricity price is comparable to driver rates or *eco-driving* is tuned to reduce traveling time, which

is likely to result in higher energy consumption. The former is briefly shown in the next subsection. The latter only requires the driver to accelerate as fast as possible, which neglects the need for speed advice.

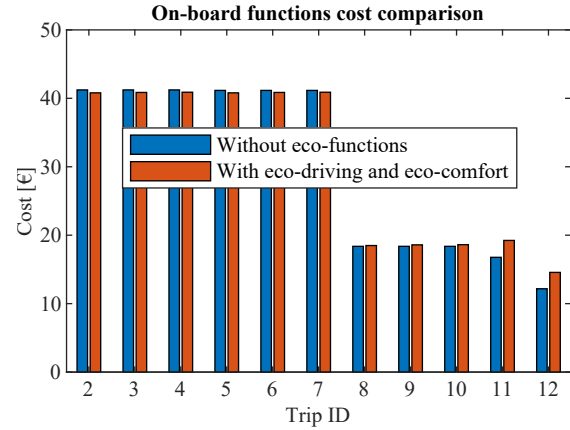


Figure 13: Cost comparison with onboard eco-functions.

### 4.3 Combined Savings Effect of the Multi-Layer EMS

The energy consumption of the complete multi-layer EMS is presented in Fig. 14. Note that in this case, the benchmark corresponds to not using any eco-function while driving the benchmark routes. Using the multi-layer EMS reduces the energy consumption in all the test cases. This is mostly due to the effect of the on-board eco-functions.

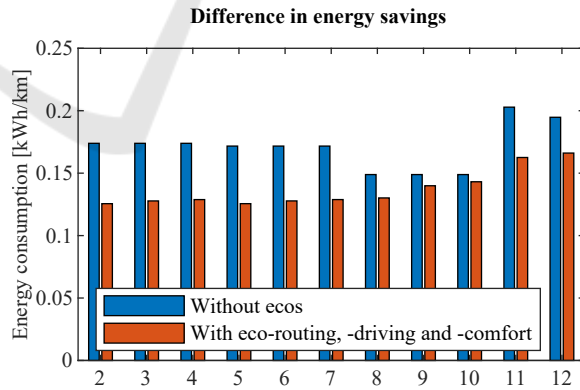


Figure 14: Energy consumption comparison with all eco-functions.

The traveling time comparison is shown in Fig. 15. As the figure shows, the traveling time is virtually the same in test cases 2-7, significantly shorter in 8-10 and longer in 11-12. This traveling time is the result of the shorter routes produced by *eco-routing* and the longer traveling time produced by *eco-driving*. Note that the total traveling time is only larger in test cases

11 and 12, where *eco-driving* increases it.

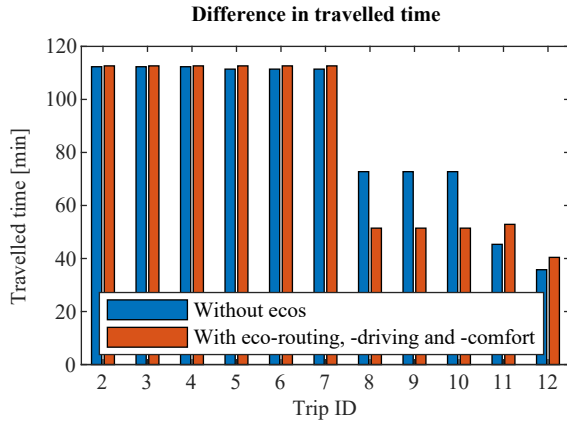


Figure 15: Travelled time comparison with all eco-functions.

Table 4 shows an overview of the resulting operational costs of using the multi-layer EMS. In most of the cases, the total operational costs are lower using the eco-functions, despite the added cost of the *eco-driving* in the vehicle layer. Following the trend of Fig. 15, the costs on test cases 11 and 12 are higher, due to the additional traveling induced by *eco-driving*.

Table 4: Cost improvement based on Eq. 14 and the costs of Section 3.5. Positive values indicate savings.

ID	On board only	Fleet only	Combined
2	1.04	9.35	5.23
3	0.89	9.15	5.04
4	0.82	9.3	5.09
5	0.87	8.44	4.67
6	0.72	8.62	4.69
7	0.65	8.39	4.53
8	-0.63	33.48	19.66
9	-1.18	33.47	19.38
10	-1.34	33.45	19.32
11	-14.72	5.28	-4.55
12	-19.64	10.6	-3.53

To show more significant savings of the multi-layer EMS, the operational costs are re-calculated using a hypothetical labor cost of  $C_d = 2[\text{€/hour}]$ , while the electricity costs are kept the same. The results are summarized in Table 5. With this reduced rate, the battery degradation and electricity price become more significant in the cost calculations. For example in the cloud functions costs, battery degradation becomes the dominant factor with the reduced hourly rate, making the relative savings higher than with a normal hourly rate. Likewise, in the on-board functions costs, electricity price becomes the dominant factor, yielding to savings in all test cases. Con-

sequently, the multi-layer EMS shows costs and energy savings in all test cases. This hypothetical rate shows that the multi-layer EMS can be cost-effective, depending on the ratio of labor and electricity prices.

Table 5: Cost improvement based on Eq. 14 and  $C_d = 2$  [€/hour]. Positive values indicate savings.

ID	On board only	Fleet only	Combined
2	24.29	26.78	25.46
3	23.64	26.1	24.78
4	23.32	26.53	24.83
5	23.72	25.66	24.62
6	23.06	26.23	24.55
7	22.74	25.41	23.98
8	25.42	28.8	27.3
9	22.98	28.57	26.05
10	22.25	28.52	25.71
11	7.08	12.01	9.59
12	4.39	11.55	8.34

## 5 CONCLUSIONS

This paper presented the operational cost and energy savings of a multi-layer Energy Management System (EMS) for a fleet of Battery-Electric Vehicle (BEV), used in distribution logistics.

The EMS is composed of fleet-layer (*eco-routing* and *eco-charging*) and vehicle-layer algorithms (*eco-driving* and *eco-comfort*). *Eco-routing* finds the route for the vehicles in the fleet, which minimizes the total traveling distance. *Eco-charging* finds a charging schedule, which minimizes battery degradation and electricity cost. *Eco-driving* provides each driver with a speed advise, that minimizes the energy consumption of the vehicle powertrain. *Eco-comfort* minimizes the energy consumption of the vehicle thermal systems, while considering driving comfort. The multi-layer EMS is tested in a case study, which simulates information about the operation of a fleet of BEVs using real traffic and weather information.

Simulation results show that on a fleet level, *eco-routing* reduces the traveling distance of the whole fleet when compared to a baseline algorithm. This in turn reduces the labour related costs due to the faster delivery times. *Eco-charging* reduces the charging-related costs because the charging operation mostly occurs when the electricity tariffs are low and because the reduced battery degradation. Both fleet-level eco-functions add their individual savings to the total fleet-level savings.

Results also show that *eco-comfort* reduces the energy consumption of the thermal systems on the ve-

hicle, depending on several factors, such as ambient temperature and algorithm settings. All energy savings of *eco-comfort* result in savings on operational costs, with a possible reduction in thermal comfort. *Eco-driving* also reduces the energy consumption of the vehicle powertrain, depending on the maximum acceleration set in the algorithm and the maximum speed. However, such a reduction comes with an additional traveling time, which increases the labor costs. The settings of *eco-driving* needs to be carefully chosen depending on the electricity price and the labor costs, to provide operational savings.

Lastly, results also show that using all the eco-functions in the multi-layer EMS results in a reduction in energy consumption in the entire fleet. However, the operational cost savings related to energy consumption are slightly reduced by the fact that *eco-charging* charges the fleet preferably when the electricity prices are lower. Likewise, the traveling time of each vehicle is increased by the effect of *eco-driving* and decreased by the effect of *eco-routing*. The benefits of these eco-functions can cancel each other if *eco-driving* is not properly tuned, leading to higher labour costs. Therefore, an additional simulation is run to show a hypothetical case in which the benefits of both *eco-driving* and *eco-routing* can be added to each other, due to the costs of energy-related savings being comparable to the labor-related savings.

## ACKNOWLEDGEMENTS

This research has received funding from the European Union's Horizon 2020 research and innovation programme under grant No 101006943, title of URBANIZED.

## REFERENCES

- Ahmadi, P. (2019). Environmental impacts and behavioral drivers of deep decarbonization for transportation through electric vehicles. *Journal of Cleaner Production*, 225:1209–1219.
- Ajanović, Z. et al. (2018). A novel model-based heuristic for energy-optimal motion planning for automated driving. 15th IFAC Symposium CTS, 51(9):255–260.
- Anosike, A. et al. (2023). Exploring the challenges of electric vehicle adoption in final mile parcel delivery. *International Journal of Logistics Research and Applications*, 26(6):683–707.
- Cataldo-Díaz, C. et al. (2024). Mathematical models for the electric vehicle routing problem with time windows considering different aspects of the charging process. *Operational Research*, 24(1):1.
- Donateo, T. et al. (2014). A method to estimate the environmental impact of an electric city car during six months of testing in an Italian city. *Journal of Power Sources*, 270:487–498.
- European Commission (2022). Hourly labour costs ranged from €8 to €51 in the EU. <https://ec.europa.eu/eurostat/web/products-eurostat-news/w/DDN-20230330-3>. Accessed:01-02-2024.
- Ewert, A. et al. (2020). Small and light electric vehicles: An analysis of feasible transport impacts and opportunities for improved urban land use. *Sustainability*, 12(19).
- Gao, Z. et al. (2023). Electric vehicle lifecycle carbon emission reduction: A review. *Carbon Neutralization*, 2(5):528–550.
- Geerts, D. et al. (2022). Optimal charging of electric vehicle fleets: Minimizing battery degradation and grid congestion using battery storage systems. In *Second International Conference SMART*, pages 1–11. IEEE.
- Han, J., Vahidi, A., and Sciarretta, A. (2019). Fundamentals of energy efficient driving for combustion engine and electric vehicles: An optimal control perspective. *Automatica*, 103:558–572.
- Kallehauge, B. et al. (2005). *Vehicle routing problem with time windows*. Springer.
- Kwak, K. H. et al. (2023). Thermal comfort-conscious eco-climate control for electric vehicles using model predictive control. *Control Engineering Practice*, 136:105527.
- Lacombe, R. (2023). Distributed optimization for the optimal control of electric vehicle fleets.
- Lera-Romero, G. et al. (2024). A branch-cut-and-price algorithm for the time-dependent electric vehicle routing problem with time windows. *European Journal of Operational Research*, 312(3):978–995.
- Medina, R. et al. (2020). Multi-layer predictive energy management system for battery electric vehicles. *IFAC-PapersOnLine*, 53(2):14167–14172.
- Medina, R. et al. (2023). Urbanized D4.4: Optimised self-adaptive, multi-layer EMS design and virtual validation fleet management algorithm. Technical report, European Union Horizon 2020, research and innovation programme.
- Naeem, H. M. Y. (2023). *Eco-driving Control of Electric Vehicle with Realistic Constraints*. PhD thesis, Capital University.
- Purnot, T. et al. (2021). Urbanized D2.1: Mission profiles, KPIs, assessment plan, List of vehicle requirements, design specifications and shared interfaces. Technical report, European Union Horizon 2020, research and innovation programme.
- Rath, S. et al. (2023). Real-time optimal charging strategy for a fleet of electric vehicles minimizing battery degradation. In *SEFET*, pages 1–8. IEEE.
- Sendek-Matysiak, E. et al. (2022). Total cost of ownership of light commercial electrical vehicles in city logistics. *Energies*, 15(22).
- Siragusa, C. et al. (2022). Electric vehicles performing last-mile delivery in B2C e-commerce: An economic and

- environmental assessment. *International Journal of Sustainable Transportation*, 16(1):22–33.
- Smith, W. J. (2010). Can EV (Electric Vehicles) address Ireland's CO<sub>2</sub> emissions from transport? *Energy*, 35(12):4514–4521.
- Zhang, L. et al. (2021). Optimal electric bus fleet scheduling considering battery degradation and non-linear charging profile. *Transportation Research Part E: Logistics and Transportation Review*, 154:102445.

